sliding terminations," *IEEE Trans. Microwave Theory Tech.*, vol. MTT-26, pp. 951–957, Dec. 1978.
[13] A. R. Kerr and Y. Anand, "Schottky-diode millimeter detectors," *Microwave J.*, vol. 24, no. 12, pp. 67–71, Dec. 1981.

✤

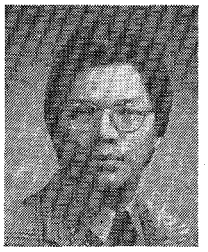

Robert A. Fong-Tom (M'74) received the B.S. degree from the Polytechnic Institute of Brooklyn, Brooklyn, NY, and the M.S. degree from Stanford University, Stanford, CA, both in electrical engineering in 1970 and 1972, respectively.

From 1972 to 1973 he was a Microwave Engineer with Desitron Co., Ltd., Ont., Canada. In 1974 he joined the Physics Department, Yale University, where he was responsible for the design of millimeter-wave and microwave systems for atomic and high-energy physics experiments. Since 1980 he has been a Member of the Technical Staff at the Sperry Research Center, Sudbury, MA, where he is currently engaged in research and development of millimeter-wave dual six-port network analyzers.

✤

Harry M. Cronson (S'58–M'64–SM'72) received the Sc.B. (summa cum laude), Sc.M., and Ph.D. degrees in electrical engineering from Brown University, Providence, RI. He also held a Keen Post-Doctoral Fellowship at Oxford University in England.

In 1964 he joined the Polytechnic Institute of Brooklyn, Farmingdale, NY, as Assistant Professor of Electrophysics. After employment with the Avco Space System Division, Wilmington, MA, and IKOR, Inc., Burlington, MA, he joined the Sperry Research Center, Sudbury, MA, in 1971 as a Member of the Technical Staff. His research interests at Sperry have included time domain metrology, short-pulse radar systems, and microwave and millimeter-wave six-port network analyzers.

A Quasi-Optical Polarization-Duplexed Balanced Mixer for Millimeter-Wave Applications

KARL D. STEPHAN, STUDENT MEMBER, IEEE, NATALINO CAMILLERI, STUDENT MEMBER, IEEE, AND TATSUO ITOH, FELLOW, IEEE

Abstract — **An integrated planar antenna-mixer structure for use at millimeter-wave frequencies is described. A simple but accurate theory of the slot-ring antenna is applied to several experimental devices. Mixer conversion loss of about 6.5 dB was obtained from an *X*-band model. Measured radiation patterns of structures designed for 65 GHz agree reasonably well with theory.**

I. Introduction

As MILLIMETER-WAVE systems increase in complexity, a strong need arises to simplify each component to the utmost extent. What may be a practical size for a single receiver front end (antenna, mixer, and associated waveguides) becomes highly impractical if one tries to build an array of such receivers. The planar structure described in this paper combines the functions of receiving antenna and balanced mixer in one simple metallized pattern on a dielectric substrate, which indeed can be the semiconductor from which the mixer diodes are formed. A working model tested at *X*-band gave a conversion loss of 6.5 ± 3 dB, and actual devices designed for use above 30 GHz yielded antenna radiation patterns which agree with the theory developed in this paper. Detailed discussion of operation will begin with the antenna structure itself.

Manuscript received May 5, 1982; revised June 21, 1982. This work was supported by U.S. Army Night Vision and Electro-optics Laboratory through the U.S. Army Research Office under Contract DAAG29-81-K-0053.

The authors are with the Department of Electrical Engineering, University of Texas at Austin, Austin, TX 78712.

II. Slot-Ring Antenna

The slot-ring antenna is one of a class of radiating structures formed from a gap or hole in an otherwise continuous metallic sheet. The sheet may or may not be backed on one side by a dielectric layer. In this paper, both the conducting sheet and the dielectric are assumed to be lossless. The slot-ring structure is the mechanical dual of the more familiar microstrip-ring resonator (see Fig. 1). The microstrip ring is a segment of microstrip bent into a loop; the slot ring is a segment of slot line bent into a loop. Slot line, first described by Cohn [1], has recently found application in millimeter-wave mixers [2]. The technique of bonding mixer diodes across the slot results in a connection with minimum stray inductance. This advantage is utilized in the mixer to be described.

0018-9480/83/0200-0164$01.00 ©1983 IEEE

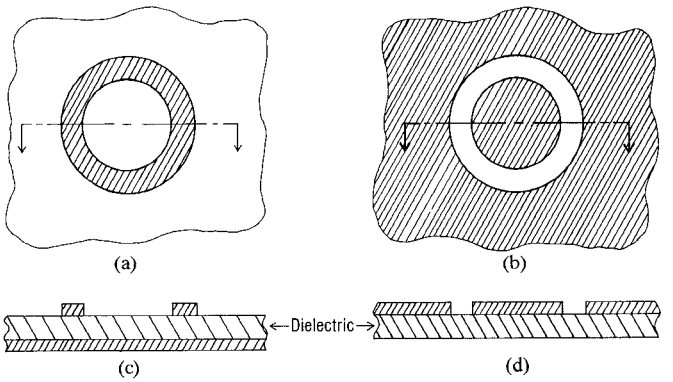

Fig. 1. Comparison of (a) microstrip-ring and (b) slot-ring structures. (c) Ground plane. (d) No ground plane.

Like the microstrip resonator, the slot-ring structure's resonant modes occur at frequencies for which the ring circumference equals an integral number of guide wavelengths. To use the structure as an antenna, the first-order mode is excited as shown in Fig. 2. Neglecting the other modes for the moment, the impedance seen by the voltage source will be real at resonance, and all the power delivered will be radiated. Three problems arise: 1) how to calculate the resonant frequency; 2) how to determine the ring's radiation pattern; and 3) how to find the input resistance at resonance.

A first-order estimate of the resonant frequency can be derived from the transmission line equivalent circuit of the slot ring (Fig. 3). By placing a magnetic wall across the ring as shown in Fig. 3(a), we disturb nothing since the structure is symmetrical. The wall permits opening the ring at the point diametrically opposite the feed, since no current flows through the wall. This operation yields the equivalent transmission-line circuit shown in Fig. 3(b).

At the resonant frequency of the first-order mode, the two lines are each a half-wave long electrically. Knowledge of the mechanical length (πr_{av}, where r_{av} is the average ring radius) and the velocity factor allows the calculation of resonance to within about 10 to 15 percent of the true frequency, even though the published tables for straight slot line [3] are used with the curved line shown in Fig. 3(a). The smaller the relative gap g/r_{av}, the better the estimate will be. For a more precise calculation, recourse can be made to spectral-domain techniques such as in the paper by Araki and Itoh [4]. Once the resonant frequency is determined for a particular application, both the radiation patterns and the impedance may be found by means of the following analysis.

In [4], Araki and Itoh showed that if the tangential electric field was known on a cylindrically symmetric planar surface, the field could be Hankel-transformed to derive the far-field radiation patterns from that surface. In their case, the fields had to be calculated from estimates of the currents on a microstrip patch. In the present case, however, a very simple estimate of the electric field in the slot will yield a good evaluation of the antenna patterns and the radiation impedance.

In choosing an estimate of the field, care should be taken to insure that the functional form is easy to Hankel-transform analytically. The estimate chosen is

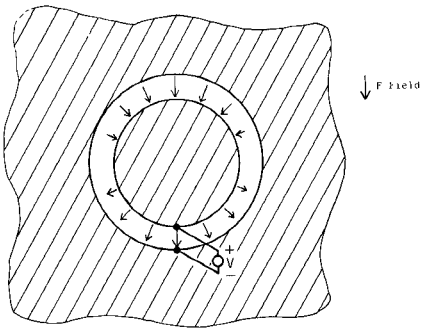

Fig 2. Slot-ring feed method showing electric field in plane of device.

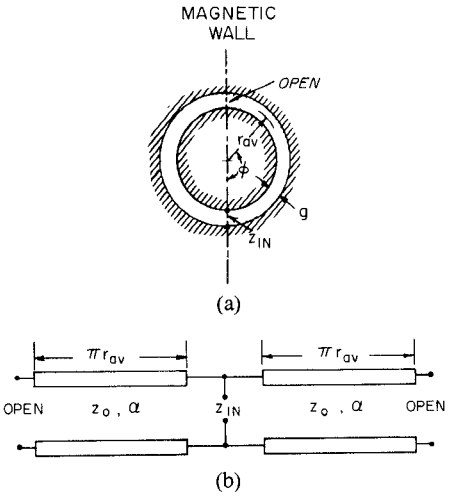

Fig. 3. Transmission-line equivalent circuit of slot-ring antenna. (a) With magnetic wall across slot ring. (b) Resulting transmission-line circuit.

$$E_r(r) = \frac{1}{r} \quad \text{for } \left(r_{av} - \frac{g}{2}\right) < r < \left(r_{av} + \frac{g}{2}\right) \tag{1}$$

$$E_r(r) = 0 \quad \text{otherwise} \tag{2}$$

$$E_\phi = 0. \tag{3}$$

This simple choice satisfies the boundary condition that the tangential electric field be zero on the metallic sheet, and expresses the intuitively reasonable idea that, for narrow gaps at least, the azimuthal field in the gap will be small compared to the radial field.

Define the $(n \pm 1)$th order Hankel transforms of the chosen function to be

$$\tilde{E}_{(\pm)}(\alpha) = \int_0^\infty E_r(r) J_{n\pm1}(\alpha r) r\, dr \tag{4}$$

where $J_n(\alpha r)$ is the nth-order Bessel function of the first kind, and α is the Hankel-transform variable. Applying this to the chosen estimate, we find

$$\tilde{E}_{(\pm)}(\alpha) = \int_{r_i}^{r_a} \frac{1}{r} J_{n\pm1}(\alpha r) r\, dr \tag{5}$$

$$\tilde{E}_{(\pm)}(\alpha) = \int_{r_i}^{r_a} J_{n\pm1}(\alpha r)\, dr \tag{6}$$

where we have called the inner and outer ring radii r_i and r_a, respectively. This integral is easy to evaluate analyti-

cally, through recursion relations given in published tables [5]. Assuming that all the fields vary as $e^{jn\phi}$, and using the saddle-point equations given in [3], we find that the far-field equations for E_θ and E_ϕ are

$$E_\theta(r,\theta,\phi) = -k_0 \frac{e^{-jk_0 r}}{r} \frac{j^n e^{jn\phi}}{2} \left[\tilde{E}_0(k_0 \sin\theta)\right] \tag{7}$$

$$E_\phi(r,\theta,\phi) = +k_0 \frac{e^{-jk_0 r}}{r} \frac{j^{n+1} e^{jn\phi}}{2} \cos\theta \left[\tilde{E}_e(k_0 \sin\theta)\right] \tag{8}$$

where linear combinations of the Hankel-transformed estimates are used

$$\tilde{E}_0(k_0 \sin\theta) = \tilde{E}_{(+)}(k_0 \sin\theta) - \tilde{E}_{(-)}(k_0 \sin\theta) \tag{9}$$

$$\tilde{E}_e(k_0 \sin\theta) = \tilde{E}_{(+)}(k_0 \sin\theta) + \tilde{E}_{(-)}(k_0 \sin\theta). \tag{10}$$

The standard spherical coordinates r, θ, and ϕ refer to the point at which the fields are measured, $r = 0$ being the center of the ring. The quantity k_0 is the wavenumber in free space $\omega\sqrt{\mu_0 \epsilon_0}$, and n is the order of resonance being analyzed. In the case of interest, $n = 1$ and $\omega = \omega_0$, the resonant frequency.

Equations (7) through (10) apply to any tangential electric field in the plane containing the origin of the spherical coordinate system. In order to treat the case of a finite thickness of dielectric, the estimated field must be transformed through the dielectric layer so that the Hankel transforms operate on the dielectric-air interface. In the Hankel-transform domain, this is a relatively easy process. Define d to be the thickness of the dielectric layer of relative dielectric constant ϵ_r.

If we let

$$\alpha = k_0 \sin\theta \tag{11}$$

$$\beta_1 = \sqrt{k_0^2 - \alpha^2} \tag{12}$$

$$\beta_2 = \sqrt{k_0^2 \epsilon_r - \alpha^2} \tag{13}$$

$$f_e(\alpha) = \frac{\beta_2 \cos\beta_2 d + j\epsilon_r \beta_1 \sin\beta_2 d}{\beta_2 \sin\beta_2 d - j\epsilon_r \beta_1 \cos\beta_2 d} \tag{14}$$

$$f_h(\alpha) = \frac{\beta_2 \sin\beta_2 d - j\beta_1 \cos\beta_2 d}{\beta_2 \cos\beta_2 d + j\beta_1 \sin\beta_2 d} \tag{15}$$

then the Hankel-transformed fields at the dielectric-air interface are given by

$$\tilde{E}_e(\alpha) = \left[\cos\beta_2 d + f_h(\alpha) \cdot \sin\beta_2 d\right] \cdot \left[\tilde{E}_{(+)}(\alpha) + \tilde{E}_{(-)}(\alpha)\right] \tag{16}$$

$$\tilde{E}_0(\alpha) = \left[\cos\beta_2 d - f_e(\alpha) \cdot \sin\beta_2 d\right] \left[\tilde{E}_{(+)}(\alpha) - \tilde{E}_{(-)}(\alpha)\right]. \tag{17}$$

Substituting these equations into (7) and (8) now gives the far-field expressions for the dielectric-coated side of the slot-ring antenna.

It should be noted that this analysis assumes that only the first-order mode is excited, and that no higher order surface waves arise. The former assumption is justified in that the zero-order mode and all higher order modes have a very small radiation impedance compared to that of the first-order mode, at its resonant frequency. The latter assumption may be justified [6] when the dielectric thickness is less than

$$d_{\max} = \frac{\pi}{2k_0\sqrt{\epsilon_r - 1}}. \tag{18}$$

Also, the equations assume that the metallic sheet extends to infinity. Practical antennas always stop short of this, but the effects of a noninfinite conductor will appear as inaccuracies only near $\theta = 90°$ (edge view of the device).

The third problem to be addressed is the radiation impedance. A classic method easily yields this result. The terminal voltage can be found by integrating the assumed field across the gap

$$|V| = \int_{r_i}^{r_a} \frac{1}{r} dr \tag{19}$$

$$|V| = \ln\left(\frac{r_a}{r_i}\right). \tag{20}$$

The total power radiated from the antenna with this voltage at its terminals is obtained [7] with the aid of (7) and (8)

$$P = \iint_{\text{sphere}} \frac{\frac{1}{2}\sqrt{|E_\theta|^2 + |E_\phi|^2}}{Z_{\text{fs}}} ds \tag{21}$$

where Z_{fs} is the intrinsic impedance of free space.

Since the input impedance Z_{in} at resonance is purely resistive, the input power at the terminals equals the radiated power

$$2 \cdot \frac{V^2}{2Z_{\text{in}}} = P. \tag{22}$$

The factor of 2 in front arises from the fact that the practical antenna is excited from only one point, but the field equations assume excitation of both orthogonal modes in quadrature ($\cos\theta + j\sin\theta$). Solving for Z_{in}, we find

$$Z_{\text{in}} = \frac{\left[\ln\left(\frac{r_a}{r_i}\right)^2\right]}{P}. \tag{23}$$

Care must be taken to use the proper equations for E_θ and E_ϕ on the dielectric and metal sides. This completes the analysis of the antenna. Strictly speaking, the resistance found in (23) applies only at the resonant frequency, although it will not vary appreciably for a small frequency range around resonance. The slot ring operated at its first-order resonance is a fairly low-Q device, so neither precise impedance calculations nor exact resonant frequencies are vital to a serviceable design.

III. Mixer Theory

Discussion of the mixer theory will be limited to explanations of the unique features embodied in the slot-ring antenna mixer.

The slot-ring antenna can support two independent

first-order modes, just as the microstrip ring resonator can. This feature allows a form of polarization duplexing in which two feed points, if separated by 90° along the ring, can couple independently to horizontally and vertically polarized waves, with little or no cross-coupling between the feeds. For exact independence, the two orthogonal feeds should each be balanced on diametrically opposite sides of the ring (four feed points altogether), but the slight imbalance caused by using only two feed points is small.

The basic operation of the mixer in a balanced, polarization-duplexed mode is illustrated in Fig. 4. The RF signal arrives as a horizontally polarized plane wave incident perpendicular to the antenna on the dielectric side. The LO signal is vertically polarized, and can arrive from either side of the structure. V_{rf} and V_{lo} show the electric field vectors on the antenna plane. By resolving each vector into two perpendicular components, it is easy to see that mixer diode D_1 receives

$$\frac{V_{lo} - V_{rf}}{\sqrt{2}}$$

while D_2 receives

$$\frac{V_{lo} + V_{rf}}{\sqrt{2}}.$$

In effect, each diode has its own independent mixer circuit, with the IF outputs added in parallel. The IF signal appears as a voltage between the central metal disc and the surrounding ground plane, and is removed through an RF choke. A double-balanced mixer with improved isolation can be made by adding two additional diodes D_3 and D_4, as indicated.

The diodes can be treated independently because each diode is at the zero-voltage node of the other diode's field pattern. To evaluate the impedance seen by a single diode, we can examine the nature of the impedance Z_{in} in Fig. 3(b). At the resonant frequency of the slot ring, the diode will see the antenna's radiation resistance, typically about 250 Ω. This impedance level is compatible with available diodes. At frequencies removed from resonance, the impedance presented to the diode will include reactance, but this variation is well-modelled by the transmission-line equivalent circuit up to the frequency at which the slot is no longer small compared to a wavelength. For narrow slots, this can be 10 to 20 times the operating frequency. In almost no other mixer structure is it so easy to calculate the impedance presented to the diode. Mixer performance is, of course, very dependent on the diode embedding impedance at RF and LO harmonic frequencies and combinations thereof. As the order of resonance increases, the slot ring becomes an increasingly poor radiating structure, so little power will be radiated in the form of higher harmonics.

The antenna-mixer can be introduced in a quasi-optical arrangement in its present form with good LO-to-RF isolation, because of the symmetry afforded by the balanced configuration. Additional improvement is easily achieved by introducing grid-type polarization filters on either side,

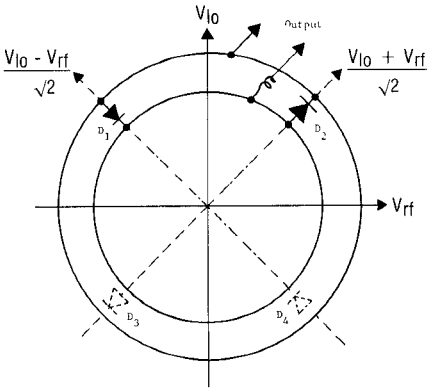

Fig. 4. Antenna-mixer showing diode input voltages.

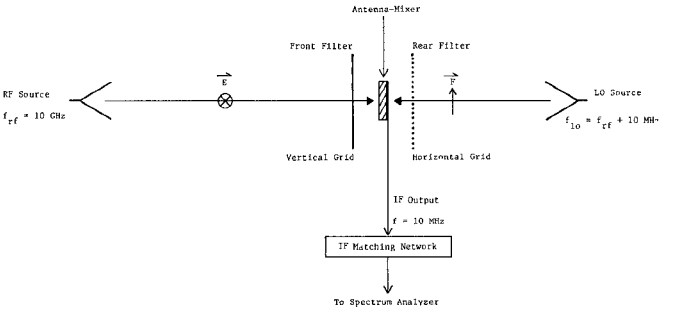

Fig. 5. Quasi-optical test setup.

as shown in Fig. 5. Horizontally polarized RF energy entering from the left passes through the front filter with little attenuation, and is received by the antenna. The rear filter is oriented to reflect the horizontally polarized RF wave, increasing directivity in the forward direction. Vertically polarized LO energy not absorbed by the antenna is blocked by the front filter and reflected back to the antenna, allowing a high degree of LO–RF isolation.

To summarize, polarization duplexing permits a balanced mixer configuration having inherently high LO-to-RF isolation. Diode embedding impedances are easy to calculate, and quasi-optical techniques can further enhance performance.

IV. Experiments

Various forms of the slot-ring structure have been constructed and measured at frequencies ranging from 400 MHz to 90 GHz. Due to equipment limitations, the only direct measures of impedance were limited to large structures below 1 GHz. These data are summarized in Table I. The calculated resonant frequencies were found using extrapolations of the published tables [3] for the $\epsilon_r = 12$ case. For the $\epsilon_r = 1$ cases, the average circumference was equated to the free-space wavelength for a first-order estimate, which turned out to be some 11-percent low. The radiation resistances were calculated using the experimentally derived resonant frequencies. Very good agreement was obtained for the $\epsilon_r = 1$ cases, and the 12-percent error for the $\epsilon_r = 12$ case is partly due to the poor mechanical contact between the metal foil used as the conducting sheet and the

TABLE I
SLOT-RING IMPEDANCE MEASUREMENTS

Structure Dimensions				Calculated Values		Measured Values		
Inner Radius (cm.)	Outer Radius (cm.)	Dielectric Constant (Relative)	Layer Thickness (cm.)	Resonant Frequency (MHz)	Radiation Resistance (ohms)	Resonant Frequency (MHz)	Radiation Resistance (ohms)	Radiation Q
7.7	8.2	1	--	600	240*	675±2	235±10	5
7.7	7.95	1	--	610	244*	676±2	232±10	6.6
3.048	3.302	12	0.635	720	590**	882±2	518±20	25.9

* At f_o = 660 MHz

** At f_o = 880 MHz

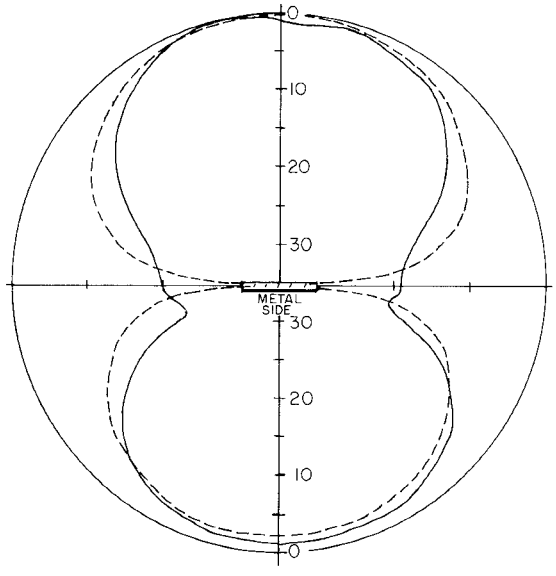

Fig. 6. Calculated and measured H-plane patterns, 10-GHz slot-ring antenna. Inner ring radius = 0.39 cm, outer ring radius = 0.54 cm, dielectric $\epsilon_r = 2.23$, thickness $d = 0.3175$ cm. All patterns are decibels down from maximum. --- Calculated.——Measured.

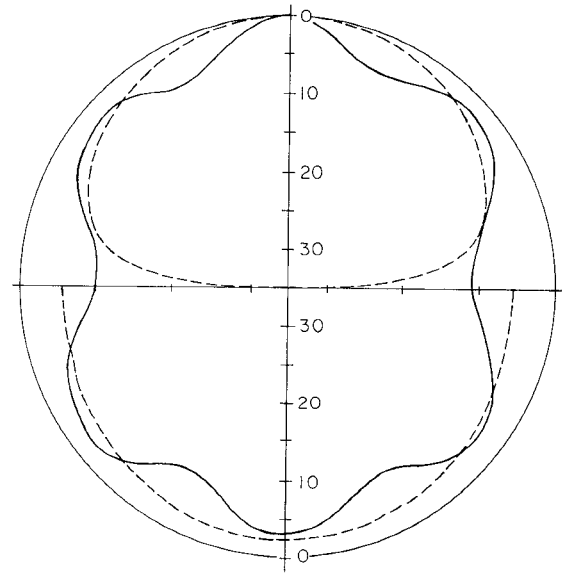

Fig. 7 Calculated and measured E-plane patterns, 10-GHz slot-ring antenna.

ceramic dielectric slab. Note that the radiation Q rises for the higher dielectric, but is still tolerably low even for a substrate having a dielectric constant near that of GaAs.

The next step taken was to build and measure a 10-GHz model antenna mixer. Calculated and measured antenna patterns are shown in Figs. 6 and 7. As anticipated, the predicted H-plane nulls in the plane of the device are partially filled in by attenuated surface waves. Overall agreement is good, especially the ratio of peak radiation intensity on the dielectric side to the metal side. An increase in either the resonant frequency or the dielectric constant will tend to pull the excitation currents to the dielectric side, increasing the field intensity there.

Using the measured antenna patterns for the 10-GHz model, an approximate directivity on the dielectric side was calculated to be 6.5 dB, which is typical of the rather broad patterns measured. The same antenna was then used to construct a balanced mixer of the type shown in Fig. 4. The mixer with its LO excitation was placed in an RF field of known intensity, and the directivity figure found above was used to calculate the actual RF power available to the mixer input, since direct measurement was impractical. The ratio of available RF input power to the measured IF output power delivered to a 10-MHz matching network gave the conversion loss reported in Table II. The 6.5 ± 3 dB figure compares not unfavorably to conventional mixer configurations. Depending on the effective diode impedance, this could be improved further with impedance-matching circuitry or different ring dimensions.

Owing to lack of a suitable local oscillator source, no actual mixer data is yet available in the millimeter-wave range, but extensive antenna patterns were measured with a single detector diode (HP 5082-2264) mounted on the ring feed point. Two different substrates were used. One was 0.3-mm-thick alumina, which was coated with a layer of gold about 2000 Å thick. Gold wire rings were used as masks to block the evaporation, forming the slot rings. The other substrate was a polymer compound with precoated copper on one side, removed mechanically to make rings. The antennas evaluated are specified in Table III, and illustrated in Figs. 8 and 9.

The alumina substrate was thin enough to avoid higher order surface waves at 65.2 GHz, its approximate design frequency. Calculated and measured patterns at this

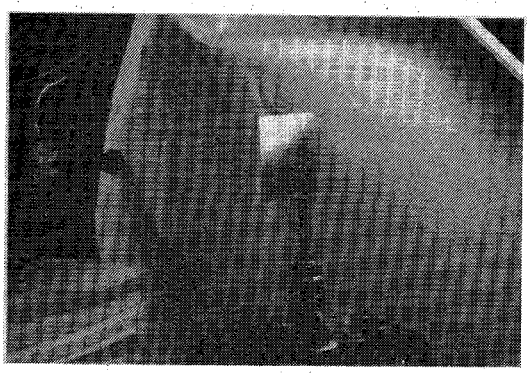

Fig. 8. Alumina substrate mounted in antenna pattern setup.

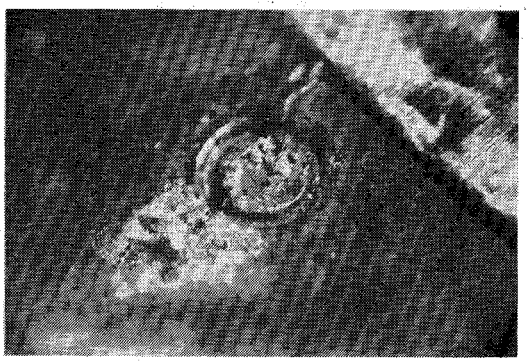

Fig. 9. Diode on plastic substrate.

TABLE II
MEASURED ANTENNA-MIXER CHARACTERISTICS

Dimensions:	Inner ring radius: 0.39 cm.
	Outer ring radius: 0.54 cm.
	Dielectric: 0.3175 cm. thick, $\epsilon_r = 2.23$
Diodes used:	NEC ND4131 ($R_s = 12$ ohms)
Antenna-mixer system:	
	RF frequency: 10 GHz
	IF frequency: 10 MHz
	RF polarization: Horizontal
	LO polarization: Vertical
	Measured conversion loss: 8 dB ± 3 dB
	LO-RF isolation: ≥ 30 dB
	RF Cross-polarization rejection: 20 dB

TABLE III
MILLIMETER-WAVE ANTENNA DIMENSIONS

	Alumina Substrate	Plastic Substrate
Dielectric Constant	9.6	2.23
Inner Ring Radius	0.0325 cm.	0.045 cm.
Outer Ring Radius	0.0375 cm.	0.070 cm.
Substrate Thickness	0.03 cm.	0.1588 cm.
Calculated Radiation Resistance	413 Ω at 65.2 GHz	390 Ω at 65.2 GHz
Substrate Size	2.9 cm. high 1.9 cm. wide	5 cm. square

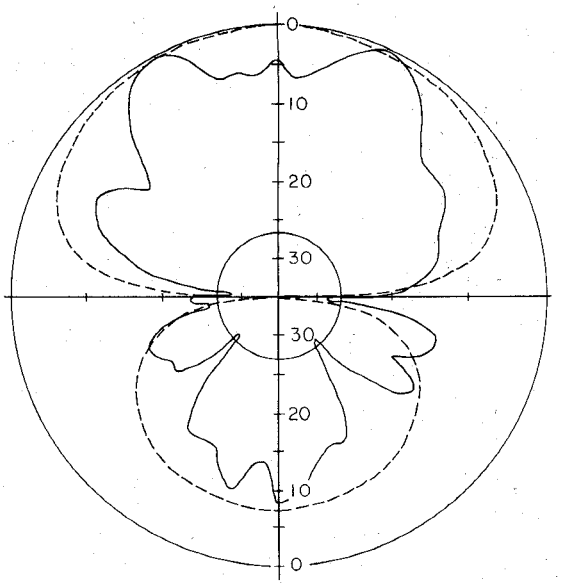

Fig. 10. Calculated and measured *H*-plane patterns, 65.2-GHz, alumina substrate. Circle indicates lower measurement limit, below which pattern is extrapolated.

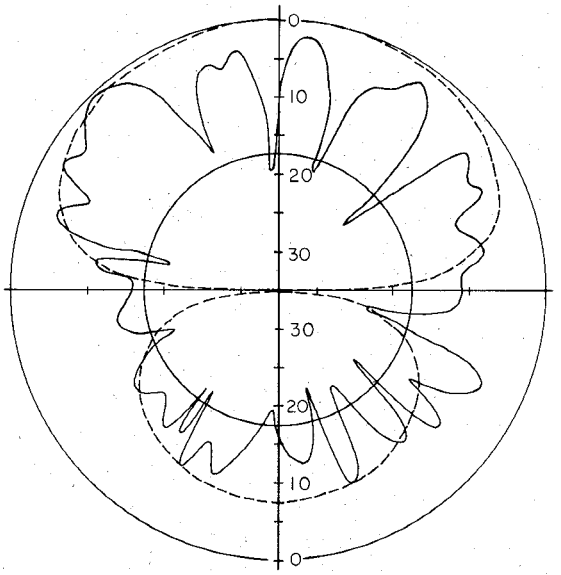

Fig. 11. Calculated and measured *H*-plane patterns, 95.5-GHz, alumina substrate.

frequency are shown in Fig. 10. Although the first-order mode radiation pattern does not predict the fine structure seen, prominent features such as the nulls in the plane of the device and the peak field values are predicted quite accurately. Compare this pattern to the one in Fig. 11, taken at 95.5 GHz. Higher order modes are evidently excited and surface waves have filled in the side nulls.

The plastic-substrate antenna was designed for 30 GHz, but equipment difficulties prevented pattern measurements in that range. The measurements of the same antenna at 65.2 GHz (Fig. 12) show effects of surface-wave excitation. The period of the nulls on the dielectric side is consistent with diffraction from the edges of the substrate itself, where surface waves emerge into the air.

Fig. 12 also shows that the feed method used does not interfere significantly with the radiation patterns. In all

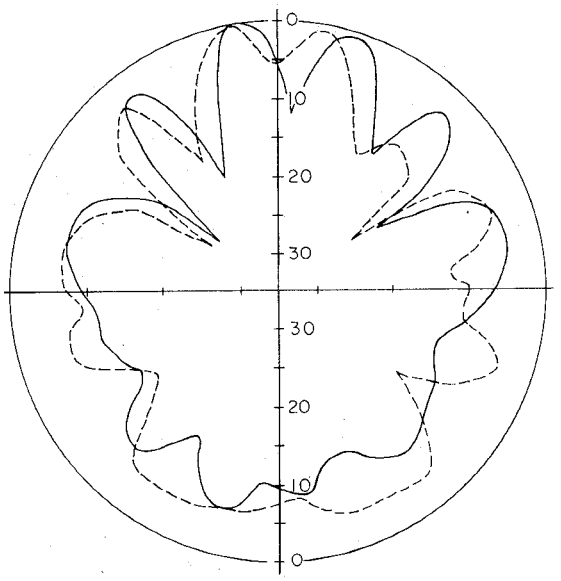

Fig. 12. Measured patterns, 65.2 GHz, plastic substrate. Dashed curve is without feed shield; solid curve is with feed shield.

other tests, the detected signal was removed from the central patch through a thin wire connected perpendicular to the device plane. After leading away from the antenna for 1–2 cm, the feed wire bends parallel to the substrate and leads to the output connector. The solid curve in Fig. 12 shows the effect of placing the insulated feed wire on the substrate and covering it with copper foil. The pattern change is relatively small, indicating that the original non-shielded feed was satisfactory. If the thin wire is not convenient mechanically, one alternative would be a coplanar line at IF, intersecting the central disc in the manner of a stick on a lollipop. A low-pass filter could be made of various sections of line with different impedances.

V. Conclusions

The slot-ring antenna-mixer has been shown to be a simple, practical component for use in quasi-optical receiving systems. A simple, but accurate, theory allows calculation of the radiation pattern and feed-point impedance, including effects of the dielectric layer. The performance of an *X*-band model was quite good for a first design attempt, and millimeter-wave measurements of structures on a high-dielectric-constant substrate indicate the practicality of forming such a device directly on a thin GaAs wafer. Arrays of such devices could open the way to phase-coherent imaging of millimeter-wave fields at a focal plane.

In addition to permitting image formation, arrays of devices will increase the overall system efficiency by presenting a larger effective aperture to typically large quasi-optical beams.

Acknowledgment

Thanks are due to L. Bui of Hughes Aircraft for providing the diodes used above 30 GHz, and to S. Sando of NEC for providing the *X*-band mixer diodes. J. Miller and Dr. R. Shurtz of the Army Night Vision and Electro-optics Laboratory provided the *X*-band detector diodes.

References

[1] S. B. Cohn, "Slot line on a dielectric substrate," *IEEE Trans. Microwave Theory Tech.*, vol. MTT-17, pp. 768–778, Oct. 1969.
[2] H. Ogawa, M. Akaike, M. Aikawa, T. Karaki, and J. Watanabe, "A 26-GHz band integrated circuit of a double-balanced mixer and circulators," *IEEE Trans. Microwave Theory Tech.*, vol. MTT-30, pp. 34–41, Jan. 1982.
[3] E. A. Mariani, C. P. Heinzman, J. P. Agrios, and S. B. Cohn, "Slot line characteristics," *IEEE Trans. Microwave Theory Tech.*, vol. MTT-17, pp. 1091–1096, Dec. 1969.
[4] K. Araki and T. Itoh, "Hankel transform domain analysis of open circular microstrip radiating structures," *IEEE Trans. Antennas Propagat.*, vol. AP-29, pp. 84–89, Jan. 1981.
[5] M. Abramowitz and I. Stegun, *Handbook of Mathematical Functions*. Washington, DC: U.S. Government Printing Office, 1972.
[6] R. F. Harrington, *Time-Harmonic Electromagnetic Fields*. New York: McGraw-Hill, 1961, p. 169.
[7] J. Kraus, *Antennas*. New York: McGraw-Hill, 1950, p. 28.

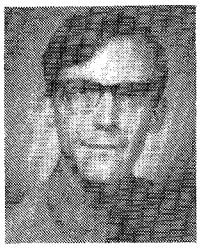

Karl D. Stephan (S'77–M'77–S'81) was born in Fort Worth, Texas, on December 18, 1953. He received the B.S. degree in engineering from the California Institute of Technology, Pasadena, CA, in 1976, and the M.Eng. Degree from Cornell University, Ithaca, NY, in 1977.

In 1977 he joined Motorola, Inc. in Fort Worth and worked in VHF and UHF mixer and filter design. From 1979 to 1981 he was with Scientific-Atlanta, Atlanta, GA, where he engaged in research and development pertaining to cable television systems. In 1981 he began graduate work at the University of Texas at Austin, where he is presently studying toward the Ph.D. degree.

Mr. Stephan is a member of Tau Beta Pi.

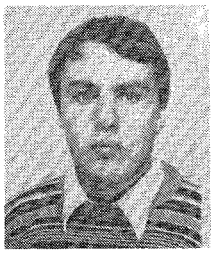

Natalino Camilleri (S'80) was born in St. Paul's Bay, Malta, on January 11, 1961. He received the B.Sc. honours degree in electrical engineering from the University of Malta in 1980, and the M.S.E. degree from the University of Texas at Austin in 1982.

He is now working as a Research Engineering Associate with the University of Texas. His current interests are low-noise millimeter-wave receivers and millimeter-wave integrated circuits.

Mr. Camilleri is a student member of IEE (London).

Tatsuo Itoh (S'69–M'69–SM'74–F'82) received the Ph.D. degree in electrical engineering from the University of Illinois, Urbana, in 1969.

From September 1966 to April 1976 he was with the Electrical Engineering Department at the University of Illinois. From April 1976 to August 1977 he was a Senior Research Engineer in the Radio Physics Laboratory, SRI International, Menlo Park, CA. From August 1977 to June 1978 he was an Associate Professor at the University of Kentucky, Lexington. In July 1978 he joined the faculty at the University of Texas at Austin, where he is now a Professor of Electrical Engineering and Director of the Microwave Laboratory. During the summer of 1979 he was a Guest Researcher at AEG-Telefunken, Ulm, West Germany.

Dr. Itoh is a member of the Institute of Electronics and Communication Engineers of Japan, Sigma Si, and Commission B of USNC/URSI. He serves on the Administrative Committee of the IEEE Microwave Theory and Techniques Society. He is a Professional Engineer registered in the State of Texas.